

Roscovitine Is an Effective Inducer of Apoptosis of Ewing's Sarcoma Family Tumor Cells *In vitro* and *In vivo*

Oscar M. Tirado, Silvia Mateo-Lozano, and Vicente Notario

Laboratory of Experimental Carcinogenesis, Department of Radiation Medicine, Georgetown University Medical Center, Washington, District of Columbia

Abstract

The Ewing's sarcoma family of tumors (ESFT) comprises several well-characterized malignant neoplasms with particularly aggressive behavior. Despite recent progress in the use of multimodal therapeutic approaches and aggressive local control measures, a substantial proportion of patients die because of disease progression. Furthermore, this outcome has not changed significantly over the last 15 to 20 years. Consequently, new, more effective therapeutic options are sorely needed for the treatment of ESFT. Because ESFT cells overexpress several cyclin-dependent kinases (CDK), we explored the efficacy against ESFT of roscovitine, a CDK inhibitor shown to be surprisingly safe for humans in clinical trials of their anticancer activity. Results showed that ESFT cell lines are uniformly sensitive to roscovitine. In addition to exerting comparatively minor cell cycle effects, roscovitine treatment concomitantly caused the up-regulation of the expression of the proapoptotic protein BAX and the down-regulation of both survivin and XIAP, thus resulting in caspase-dependent apoptosis. Furthermore, *in vivo* experiments showed that s.c. growth of ESFT xenografts was also significantly slowed by i.p. injection of roscovitine. These results strongly suggest that roscovitine may be an effective therapeutic agent against ESFT and recommend its evaluation against ESFT in clinical trials and its inclusion in future treatment protocols. (Cancer Res 2005; 65(20): 9320-27)

Introduction

Ewing's sarcoma family of tumors (ESFT), which includes Ewing's sarcoma (EWS), Askin's tumor, and primitive neuroectodermal tumors (PNET), are the second most common bone tumors in children, adolescents, and young adults (1). These tumors are characterized by the presence, in over 90% of the cases, of a balanced translocation between human chromosomes 11 and 22 that joins the 5' end of the *EWS* gene and the 3' end of the *FLI1* gene. The resulting hybrid gene encodes the EWS/FLI1 fusion protein, which has been shown to be responsible for the malignant properties of ESFT (1). Despite aggressive combinations of chemotherapy, radiotherapy, and surgery, ~50% of patients eventually relapse, even after 5 years, and >30% of patients with

localized disease and ~80% of patients with metastatic disease die due to disease progression (2). Although recently reported experimental evidence (3, 4) compellingly supports the introduction of promising, alternative therapeutic approaches for ESFT, new, more effective treatment options are sorely needed.

Molecular analyses have shown that, like most other human tumors (5, 6), ESFT frequently carry mutations in cell cycle regulators, including overexpression of cyclin D1 (7–10); elevated expression of cyclin-dependent kinase 2 (CDK2; ref. 11); losses or low expression of CDK inhibitors, such as p16^{Ink4}, p21^{WAF1}, or p27^{KIP1} (12–14); and other chromosome 9 abnormalities (15, 16). Reversion of some of these alterations after forced down-regulation of EWS/FLI-1 strongly suggested that G₁-S regulatory genes may work downstream of EWS/FLI-1 and that imbalances in their expression may contribute to tumorigenesis (1). Furthermore, an association has been detected between elevated expression of CDK2 and high risk/poor prognosis Ewing's sarcoma (11). This finding is particularly important because CDK2 inhibition has become recently an attractive therapeutic approach (5, 17, 18). Indeed, inhibitors such as roscovitine (CYC202, Seliciclib, R-roscovitine) have been shown not only to inhibit the kinase activities of the CDK2/cyclin A and CDK2/cyclin E complexes with high specificity and potency (17, 18), but are also proving unexpectedly safe for humans in clinical trials of their anticancer activity (19–22). In addition, several lines of evidence showed that CDK inhibitory drugs induce apoptosis of tumor cells (5). Roscovitine has been reported to induce apoptosis of a variety of established tumor cell lines in culture and in tumor xenografts (19, 23–26). Because tumors with dysfunctional CDK inhibitors, a known characteristic of ESFT cells (12–14, 27, 28), have been reported to be especially susceptible to CDK inhibition (5, 29), it seemed extremely likely that ESFT cells may be highly sensitive to CDK inhibition. Consequently, we tested the effect of roscovitine on EWS and PNET cells in culture and in nude mice xenografts. Results of the present study show that roscovitine is indeed a very efficient inducer of apoptosis of ESFT cells, via a mechanism involving caspase activation and the up-regulation of Bax protein expression and has a potent antitumor activity. Therefore, our data strongly suggest that roscovitine may be a useful therapeutic agent for the treatment of ESFT.

Materials and Methods

Culture conditions, antibodies, and general reagents. A4573 and SK-ES-1 cells were obtained from Dr. Timothy J. Kinsella (University Hospitals of Cleveland, OH). TC-71 cells were obtained from Dr. Jeffrey A. Toretsky (Georgetown University Medical Center, Washington, DC). TC32, SK-N-MC, and SK-N-SH cells were obtained from American Type Culture Collection (Manassas, VA). SK-ES-1, A4573, and SK-N-MC cells were maintained in DMEM (Biosource, Camarillo, CA) supplemented with penicillin, streptomycin, and 10% fetal bovine serum (Life Technologies, Gaithersburg, MD). SK-N-SH, TC-32, and TC-71 cells were maintained in RPMI 1640 (Biosource) with the same supplements. Cells were maintained at 37°C

Note: O.M. Tirado and S. Mateo-Lozano contributed equally to this work. S. Mateo-Lozano is a registered student in the Ph.D. Doctorate Program in Biochemistry and Molecular Biology of the Universitat Autònoma of Barcelona, Barcelona, Spain.

Requests for reprints: Vicente Notario, Laboratory of Experimental Carcinogenesis, Department of Radiation Medicine, Georgetown University Medical Center, Room E215, Research Building, 3970 Reservoir Road, Northwest, Washington, DC 20057-1482. Phone: 202-687-2102; Fax: 202-687-2221; E-mail: notariov@georgetown.edu.

©2005 American Association for Cancer Research.
doi:10.1158/0008-5472.CAN-05-1276

in a humidified atmosphere of 5% CO₂ and 95% air. Polyclonal antibodies against Bax, cleaved caspase-3, cleaved caspase-9, and survivin were from Cell Signaling Technology (Beverly, MA). Monoclonal XIAP antibody was from BD PharMingen (Palo Alto, CA). β -Actin (Abcam, Ltd., Cambridge, United Kingdom) detection was used as loading reference. Oligonucleotide primers were purchased from Bio-Synthesis (Lewisville, TX). Roscovitine was purchased from EMD Biosciences, Inc. (San Diego, CA) or LC Laboratories (Woburn, MA). Trypan blue was obtained from Life Technologies (Grand Island, NY). All other general reagents were from Sigma-Aldrich (St. Louis, MO).

Apoptosis and cell cycle assays. Apoptosis was evaluated by viable cell counting and/or terminal deoxynucleotidyl transferase-mediated nick end labeling (TUNEL) assays. Cell viability was determined by the trypan blue exclusion method: Cells were suspended in 0.04% trypan blue in PBS, placed on a hemocytometer, and counted under the microscope. TUNEL assays were done for the *in situ* detection of apoptotic cells using the red-based TMR *In situ* Death Detection kit from Roche Diagnostics (Indianapolis, IN). Cells were cultured in chamber slides (Nunc, Naperville, IL) to a population density of 5×10^4 cells. Sixteen hours after roscovitine exposure, cells were washed with PBS, fixed in freshly prepared paraformaldehyde (4% in PBS) for 30 minutes at room temperature, rinsed thrice in PBS, permeabilized with 0.2% Triton X-100 in PBS for 30 minutes, and incubated with the TUNEL reaction mixture for 1 hour at 37°C in a humidified atmosphere in the dark. TUNEL-positive cells were visualized with a Nikon E600 fluorescence microscope. For cell cycle analysis, cells were harvested 24 hours after exposure to roscovitine, washed once in PBS, fixed in citrate buffer (pH 7.6), resuspended in PBS containing 20 μ g/mL of propidium iodide (Calbiochem-Novabiochem Corp., San Diego, CA), and incubated for 30 minutes at 37°C before flow cytometric analysis on a FACScan instrument (Becton Dickinson, San Jose, CA), done at the Flow Cytometry/Cell Sorting Shared Resource of the Vincent T. Lombardi Comprehensive Cancer Center. The same *in situ* death detection kit was used for TUNEL assays done on deparaffinated 5 μ m tumor sections.

Caspase assays. Cultures of TC-71 and A4573 cells were established by plating either 2×10^4 cells per well in 96-well tissue culture plates (for caspase activity determinations) or 2×10^5 cells per well in six-well plates (for apoptosis assays). After overnight incubation, cells were treated for 24 hours with either 10 μ mol/L roscovitine, 5 μ g/mL cisplatin (as a positive inducer of caspase-3-dependent apoptosis), or DMSO vehicle (as the negative control), each in the presence or absence of the Ac-DEVD-CHO caspase-3/7 inhibitor at a 20 μ mol/L final concentration. All treatments were done in triplicate. Following treatment, the extent of apoptosis induction was determined as described above, and caspase-3/7 activity determinations were carried out using the Apo-ONE Homogeneous Caspase-3/7 Assay (Promega, Madison, WI) following the manufacturer's protocol. Briefly, once the reagent and the cell culture plates had been equilibrated to room temperature, an equal volume of reagent was added directly to the cell cultures, the plates were shaken at 500 rpm, and the fluorescent output was determined 8 hours after adding the reagent in a fluorescent plate reader with a 485/535 excitation/emission filter and a gain setting of 25.

Western blot analysis. Cells were lysed in radioimmunoprecipitation assay buffer containing protease inhibitors (1 mmol/L phenylmethylsulfonyl fluoride, 10 mg/mL aprotinin, and 10 mg/mL leupeptin) and the lysates were centrifuged at $13,000 \times g$ at 4°C for 30 minutes. Protein content in the supernatants was determined with the BCA protein assay system (Pierce, Rockford, IL). Proteins (40 μ g) in cell extracts were resolved by 10% SDS-PAGE and transferred to nitrocellulose membranes. After blocking with 5% nonfat dry milk in PBS containing 0.2% Tween 20, membranes were incubated at 4°C overnight with the different antibodies. Blots were then incubated for 1 hour at room temperature with horseradish peroxidase-conjugated secondary antibody (1:2,000) and the peroxidase activity was analyzed with the ECL chemiluminescence substrate system (Amersham Biosciences, Piscataway, NJ).

Immunofluorescence. Cells were grown in chamber slides, fixed, and permeabilized as described for TUNEL assays. Permeabilized cells were then incubated for 30 minutes at room temperature with 10% donkey serum in PBS to block nonspecific binding. After thorough rinsing with PBS, cells were incubated for 1 hour at 37°C with anti-cleaved caspase-3 antibody followed

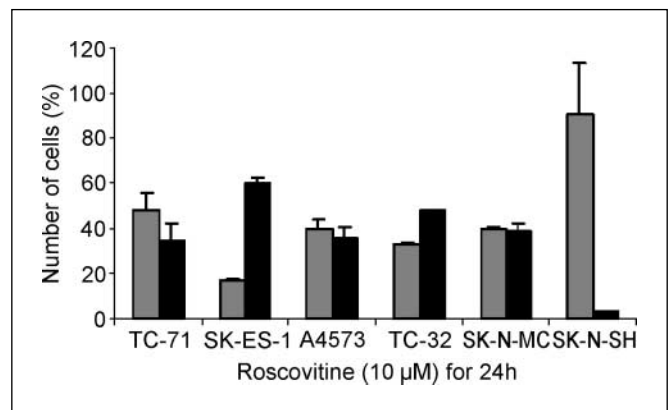


Figure 1. Roscovitine induces cell death in ESFT cultures but not in neuroblastoma cells. Exponentially growing cultures of the cell lines shown were treated with roscovitine, at the indicated concentration, for 24 hours. Then, viable and dead cell numbers were determined using the trypan blue exclusion assay. Experiments were carried out thrice, with triplicate cultures each time. Columns, mean; bars, SD. Roscovitine did not affect neuroblastoma cells (SK-N-SH cell line), while inducing substantial levels of cell death in ESFT cell cultures (all other cell lines). \square , Viable cells; \blacksquare , Dead cells.

by 30 minutes at 37°C with FITC-coupled anti-rabbit antibody. Cells were rinsed again with PBS and twice with distilled water, and mounted in Vectashield medium for fluorescence with 4',6-diamidino-2-phenylindole (DAPI; Vector Laboratories, Burlingame, CA), which provided nuclear counterstaining and visualized using a Nikon E600 fluorescence microscope. Appropriate controls were maintained by substituting the primary antibody with normal donkey and/or rabbit serum to check for nonspecific binding.

In vivo studies. Male athymic nude mice (5-6 weeks old) were obtained from the National Cancer Institute. Mice were housed in the animal facilities of the Georgetown University Division of Comparative Medicine. All animal work was done under protocols approved by the Georgetown University Animal Care and Use Committee. Mice were inoculated s.c. into the right posterior flank with 4×10^6 A4573 cells in 100 μ L of Matrigel basement membrane matrix (Becton Dickinson). Xenografts were grown to a mean tumor volume of 129 ± 30 mm³. Roscovitine was first dissolved in either absolute methanol or DMSO (1 volume). A carrier solution was produced by using a diluent containing 10% Tween 80, 20% *N,N*-dimethylacetamide, and 70% polyethylene glycol 400 (Fisher Scientific, Pittsburgh, PA). Mice were randomized into two groups (six animals per group) and treatment was initiated. One group was treated with roscovitine, administered as a single daily i.p. injection, at a dose of 50 mg/kg, for either 5 days or two 5-day series with a 2-day break in between. The control group received i.p. injections of the carrier solution following identical schedules. All mice were sacrificed by asphyxiation with CO₂. Roscovitine-treated mice were euthanized either 7 days after the first injection or up to 4 weeks after completion of the treatment. At those times, tumors were removed, measured, and prepared for TUNEL assays. Primary tumor volumes were calculated by the formula $V = (1/2)a \times b^2$, where a is the longest tumor axis and b is the shortest tumor axis. Data are given as mean values \pm SE in quantitative experiments. Statistical analysis of differences between groups was done by a one-way ANOVA followed by an unpaired Student's *t* test.

Immunohistochemistry. All tumors and tissues were fixed in 4% paraformaldehyde and embedded in paraffin. Sections (5 μ m) were stained with H&E, assayed for apoptosis by TUNEL as described above, or assessed for expression of cleaved caspase-3, using a rabbit polyclonal anti-cleaved human caspase-3 (Cell Signaling) at a 1:50 dilution, and the ABC peroxidase labeling procedure (DakoCytomation California, Inc., Carpinteria, CA) for immunologic detection.

Results and Discussion

Treatment of exponentially growing cultures of three EWS (TC-71, SK-ES-1, and A4573) and two PNET (SK-N-MC and TC-32) cell

lines with roscovitine (10 $\mu\text{mol/L}$) for 24 hours led to a strong inhibition of cell proliferation (above 60%) and the promotion of substantial levels of cell death (>35%) in all cases, relative to cultures incubated with solvent alone (Fig. 1). In contrast, no remarkable effects (<10% inhibition of cell proliferation and

apoptotic levels nearly indistinguishable from background) were observed in cultures of similarly treated SK-N-SH neuroblastoma cells (Fig. 1), thus supporting the specificity of the inhibitory action of roscovitine on ESFT cells. Although a previous study reported sensitivity of neuroblastoma cells to roscovitine treatment (29),

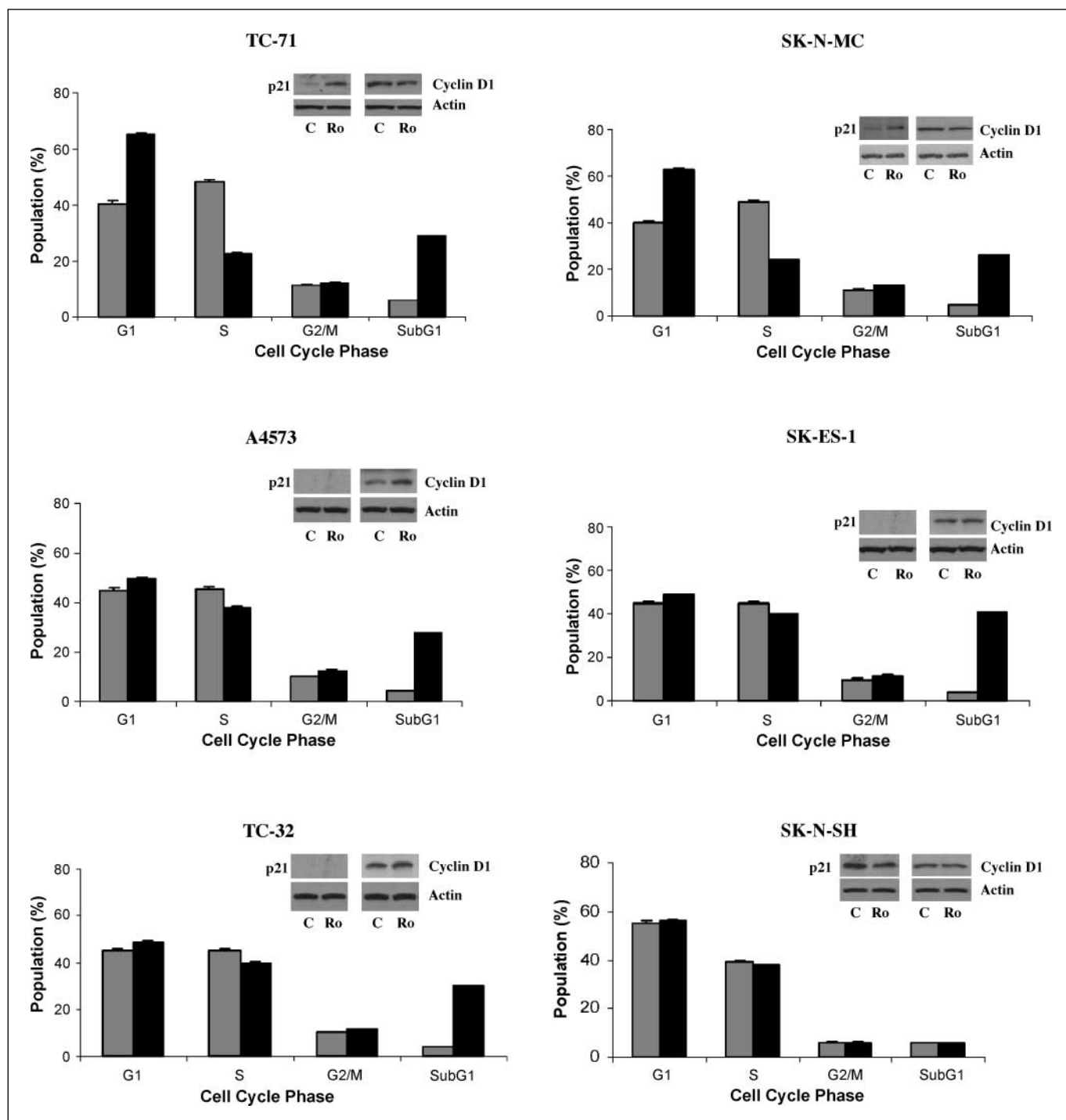


Figure 2. Cell cycle effects of roscovitine treatment. Exponentially growing cultures of the cell lines shown were treated with 10 $\mu\text{mol/L}$ roscovitine. Then, cells were stained with propidium iodide and their DNA content was determined by flow cytometry. Columns, relative percentages (mean values) of the roscovitine-treated (black columns) and untreated, control (gray columns) cell populations that could be assigned to cell cycle phases or to the sub-G₁ stage, a commonly used indicator of apoptosis; bars, SD. Experiments were carried out thrice, with triplicate cultures each time. Cells harvested from the same roscovitine-treated (Ro) and control (C) cultures were lysed, and expression of the p21^{WAF1} protein (p21) and cyclin D1 were examined by Western immunoblot analyses with specific antibodies, using actin as loading control (insets).

it must be pointed out that the inhibitor dose used in that study was 5-fold greater than that used in our experimental protocols.

To further understand the mechanism of roscovitine inhibition of ESFT cell proliferation, we analyzed the cell cycle distribution of the ESFT and neuroblastoma cell lines after treatment with roscovitine (10 $\mu\text{mol/L}$) for 24 hours. Relative to untreated controls, results showed a noticeable induction of G₁-phase arrest (up to 30%) in TC-71 and SK-N-MC cells, whereas only very slight G₁ phase changes were observed for the other ESFT cells and the neuroblastoma SK-N-SH cells (Fig. 2). No significant G₂-M arrest was observed in any of the cells tested. Interestingly, the fact that G₁ arrest was observed only in TC-71 and SK-N-MC cells correlates with the ability of these cells, but lacking in all the others, to up-regulate the levels of p21^{WAF1} protein in response to roscovitine (Fig. 2, *left insets*). Whether there is any association between this response and the fact that TC-71 and SK-N-MC were the only ones among the cell lines tested that carry a type 1 EWS/FLI-1 translocation (4) remains to be elucidated. To investigate the possible involvement of cyclin D1 in the observed cell cycle response to roscovitine treatment, cyclin D1 expression levels were examined in roscovitine-treated cells and in untreated controls. Results showed that, contrary to the reduction observed in cell lines derived from other tumor types (17), roscovitine did not cause any remarkable change in cyclin D1 levels in any of the cell lines tested (Fig. 2, *right insets*). Nevertheless, in agreement with the cell death data shown in Fig. 1, a sizable accumulation of cells in the sub-G₁ fraction (around 25%), which is suggestive of apoptotic death, was observed for all ESFT cells, but not for the neuroblastoma SK-N-SH cells (Fig. 2).

Taking into account the sub-G₁ information from the fluorescence-activated cell sorting analysis, together with the fact that roscovitine has been reported to induce apoptosis in various cancer cell lines (19, 23–26, 30, 31) and to sensitize cells to radiation (32) and chemotherapy-induced apoptosis (33) both *in vitro* and *in vivo*, we did TUNEL assays to explore the possibility that ESFT cells were undergoing apoptosis after roscovitine exposure. Results (Fig. 3) showed that, indeed, roscovitine induced apoptotic cell death in TC-71 and A4573 cells, but not in SK-N-SH cells. Moreover, results from experiments combining TUNEL assays with immunofluorescence using a specific antibody against the cleaved form of human caspase-3 strongly suggested that the apoptotic process induced by roscovitine was caspase-3 dependent (Fig. 3, *Cleaved-C3*). Quantification of the proportion of cells positive for caspase-3 cleavage (36 \pm 5.01% for TC-71; 38 \pm 3.62% for A4573; 3 \pm 0.8% for SK-N-SH) showed an excellent correlation not only with TUNEL data (Fig. 3), but also with the proportions of dead cells described for each cell line in Fig. 1. The mechanism by which roscovitine induces apoptosis is not well established, although involvement of proapoptotic members of the Bcl-2 family of proteins, such as Bcl-xS, Bax, and Bak, has been suggested (24, 34). Results from Western immunoblot analyses strongly suggested that up-regulation of Bax protein levels is an important event in roscovitine-induced ESFT apoptosis. As shown in Fig. 4A, Bax was markedly up-regulated (by as much as 2.8-fold in TC-32 cells) after roscovitine treatment in each of the three ESFT cell lines tested, whereas Bax levels were actually decreased by \sim 50% in SK-N-SH neuroblastoma cells. Furthermore, in agreement with the immunofluorescence data (Fig. 3), cleaved caspase-9 (data not

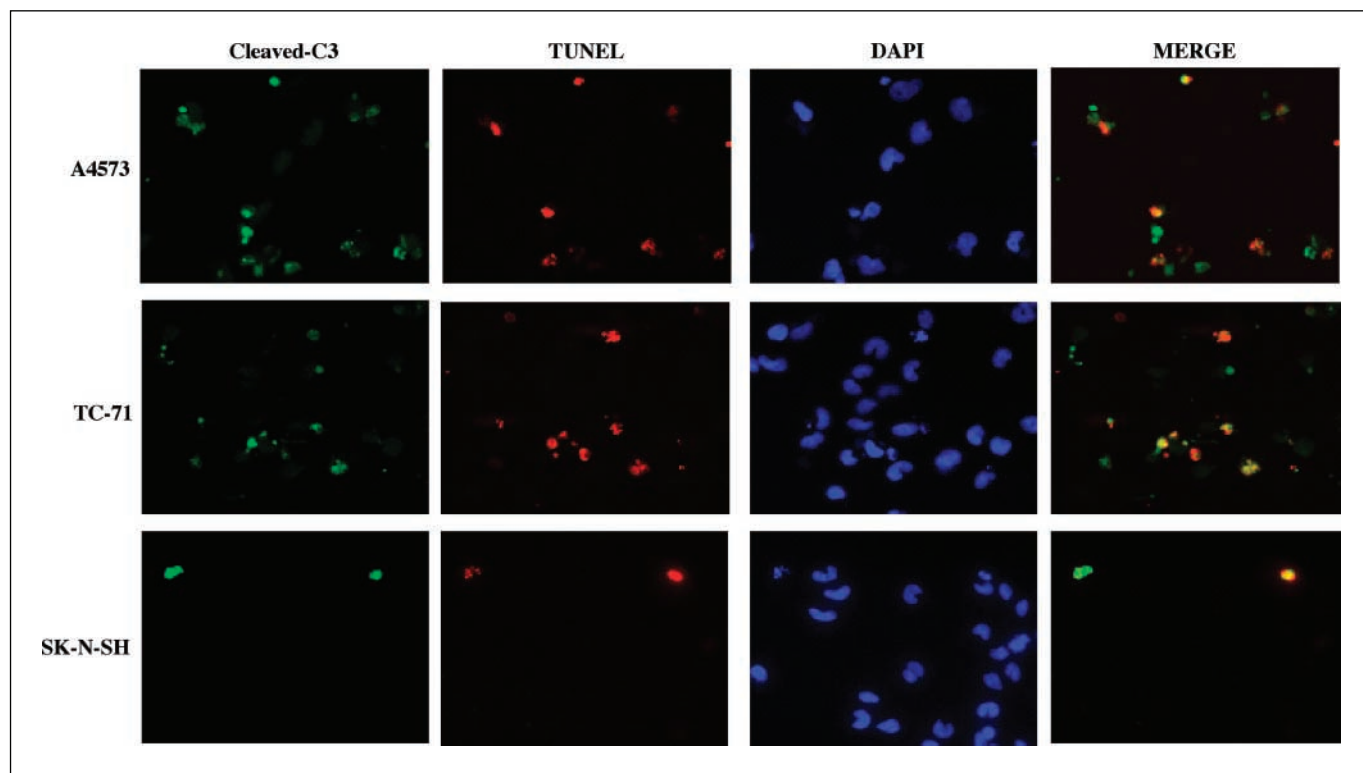


Figure 3. Roscovitine-induced apoptosis of ESFT cells involves cleavage of caspase-3. ESFT (A4573 and TC-71) cells and neuroblastoma SK-N-SH cells were grown in slide chambers and treated with 10 $\mu\text{mol/L}$ roscovitine for 16 hours. Then, apoptosis was examined by TUNEL assays (*red*), caspase-3 cleavage (visualized as green immunofluorescence using a specific antibody to the cleaved caspase-3 polypeptide form), and nuclear morphology (after DAPI staining). Merge of red and green fluorescent signals indicated that caspase-3 cleavage occurred during the apoptotic process induced by roscovitine in the ESFT cells, but not in the neuroblastoma cells.

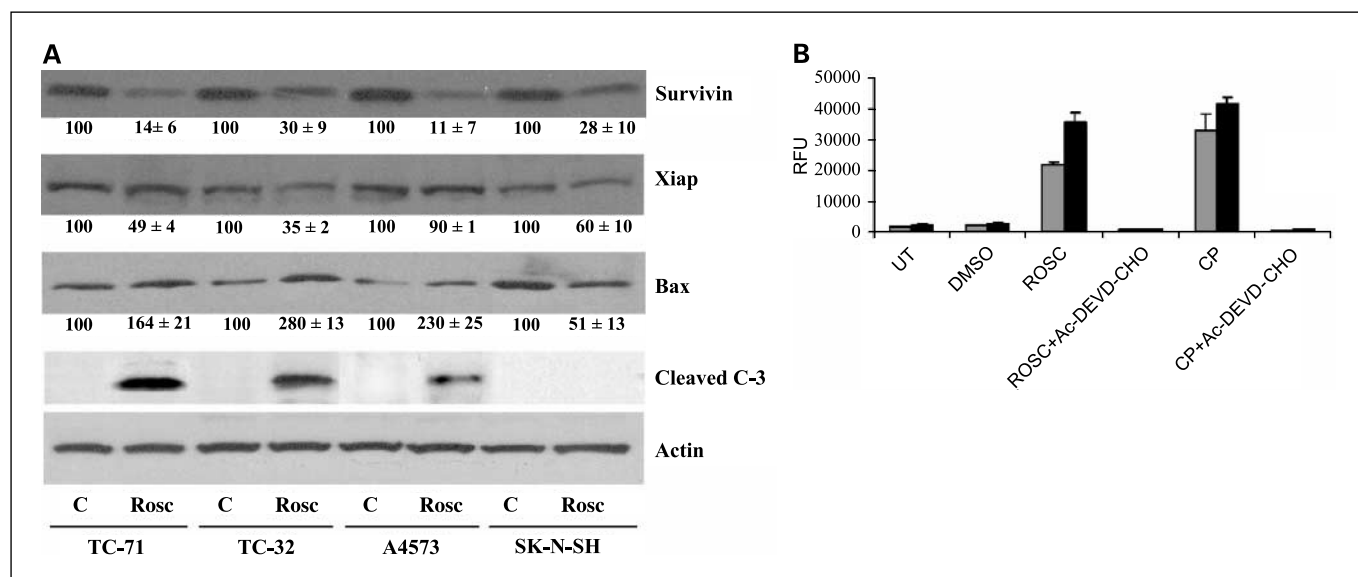


Figure 4. Roscovitine induces apoptosis in ESFT cells by concomitant up-regulation of the Bax protein and activation of caspase-3. **A**, ESFT (TC-71, TC-32, A4573) cells and SK-N-SH neuroblastoma cells were treated with 10 μ M roscovitine for 24 hours, lysed, and protein levels of surviving, XIAP, Bax, and cleaved caspase-3 were analyzed by Western immunoblot using specific antibodies. Actin was used as the loading control. A representative blot is shown for each protein. Experiments were carried out thrice, with triplicate cultures each time. The relative densitometric intensities of the signals (mean value \pm SD) from extracts of control (C) and roscovitine-treated (Rosc) cells are shown under the corresponding bands. **B**, the apoptotic process induced by treatment of the cells lines indicated with roscovitine (ROSC) was blocked by the simultaneous addition of Ac-DEVD-CHO, a caspase-3/7-specific inhibitor, to the cultures (+Ac-DEVD-CHO columns). The extent of apoptosis inhibition correlated well with the magnitude of the inhibitory effect of Ac-DEVD-CHO on the caspase-3/7 enzymatic activity in the same cells. Cisplatin (CP)-treated cells were used as positive controls for caspase-dependent apoptosis, whereas untreated cells (UT) and cells exposed to solvent alone (DMSO) were used as negative controls. \square , A4573; \blacksquare , TC-71.

shown) and cleaved caspase-3 polypeptides were observed (Fig. 4A) only in extracts of those cells in which the Bax protein was up-regulated by roscovitine, but were undetectable in SK-N-SH cell extracts. In agreement with what was previously observed in other human tumor cell types, such as chronic lymphocytic leukemia (24), the levels of proteins of the IAP family, such as Survivin and XIAP, were significantly down-regulated after roscovitine treatment in all cell lines tested (Fig. 4A). However, the absence of caspase cleavage in SK-N-SH cells strongly suggested that Bax up-regulation is a necessary requisite for the induction of apoptosis by roscovitine.

Furthermore, in agreement with results reported previously on the effect of roscovitine on human B-CLL cells (24), the caspase-3/7 dependence of the apoptotic process induced on ESFT cells by roscovitine was shown by the fact that apoptosis was blocked by treatment with Ac-DEVD-CHO, a caspase-3/7-specific inhibitor. The extent of apoptosis induced by treatment of TC-71 (42.4 ± 0.1 %) and A4573 (41.7 ± 2.3 %) cultures with roscovitine was markedly reduced when the treatment was carried out in the presence of Ac-DEVD-CHO (Table 1), which essentially prevented the apoptotic action of roscovitine and kept the proportions of apoptotic cells in the cultures at about background levels (Table 1). The decrease in roscovitine-induced apoptotic levels caused by Ac-DEVD-CHO was consistent with the reduction in the apoptotic effect caused in the same cells by cisplatin (Table 1), a known inducer of caspase-dependent apoptosis in ESFT and other cell types (35, 36), and with the extent of inhibition of the caspase-3/7 enzymatic activity induced by the inhibitor in TC-71 and A4573 cells (Fig. 4B). These results showed that the apoptotic process induced by roscovitine in ESFT cells was dependent, at least in part, on caspase-3/7 activation.

Because it has been suggested that roscovitine induces apoptosis by activating the p53 pathway (37), and Bax is a well-

known transcriptional target of p53, we analyzed the mRNA levels of Bax after treatment with roscovitine by reverse transcription-PCR. No transcriptional activation of Bax was observed in any of the cells included in this study (data not shown), perhaps as a result of the transcriptional inhibition caused by the reported effect of roscovitine on the loss of RNA polymerase II phosphorylation and total protein levels (17, 25, 38), suggesting that roscovitine treatment causes Bax up-regulation in ESFT cells at the posttranscriptional level by mechanisms involving either posttranslational modification or protein stabilization, such as those described in other experimental systems (39). These results are consistent with the fact that the ESFT cell lines used in this study have mutated or null p53 protein. Additionally, the fact that no up-regulation of Bax mRNA was detected in SK-N-SH cells, which express wild-type p53, suggest that roscovitine did not cause p53 activation in any of the cell lines tested, and that the apoptotic process triggered by roscovitine in ESFT cells is p53 independent. Although the precise molecular mechanism of Bax up-regulation mediated by roscovitine in ESFT cells remains to be elucidated, it seems clear that its overall inhibitory effect on cell proliferation *in vitro* primarily results from the efficient induction of apoptotic cell death, which in some cases may take place with the concomitant induction of G₁ phase cell cycle arrest.

We subsequently investigated the effect of roscovitine *in vivo* by evaluating the effect of drug treatment on tumor growth using nude mice xenografts of A4573 ESFT cells generated as described under Materials and Methods. When tumors reached a volume of ~ 130 mm³, animals were injected i.p. with roscovitine or with the carrier solution alone, following different schedules, and tumor growth was measured over a period of up to several weeks. As can be seen in Fig. 5A, tumor growth was significantly slower

Table 1. Effect of caspase-3/7 inhibition on the apoptotic action of roscovitine on EWS cells

Treatment	EWS cell line	
	TC-71	A4573
UT	7.4 ± 1.2	8.9 ± 0.6
DMSO	6.7 ± 3.1	10.8 ± 0.3
ROSC	42.4 ± 0.1	41.7 ± 2.3
ROSC + Ac-DEVD-CHO	5.8 ± 0.5	9.2 ± 4.0
CP	39.9 ± 1.4	32.3 ± 3.8
CP + Ac-DEVD-CHO	9.2 ± 3.4	7.5 ± 2.0

NOTE: Results are given as percentage of apoptotic cells 24 hours after the indicated treatments and correspond to mean ± SD.

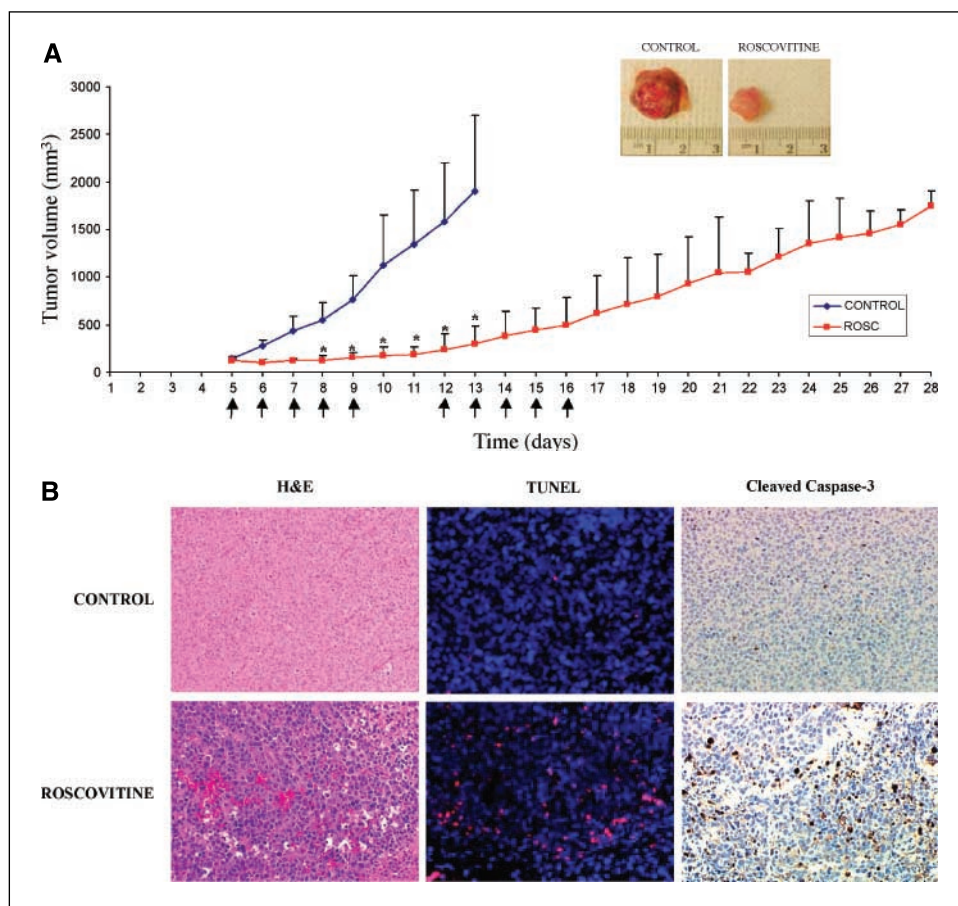
Abbreviations: UT, untreated cells; ROSC, roscovitine; CP, cisplatin.

in roscovitine-treated mice than in control animals, as a reflection of the markedly smaller size of individual tumors observed after excision (Fig. 5A, *inset*). One day after completion of the first 5-day treatment series, tumors in roscovitine-treated animals had grown only ~1.25-fold relative to their size at the time of treatment initiation, whereas tumors in untreated mice had already attained a volume ~14.5-fold their original size. These values represented a difference of ~11.5-fold in tumor volume

and, although tumors in roscovitine-treated animals continued to grow very slowly, a significant difference (~7.5-fold) in tumor size was still evident at the time (day 13; Fig. 5A) when control animals, whose tumors had grown to ~15-fold their initial size, had to be sacrificed following Institutional Animal Care and Use guidelines. Counting from day 1 of roscovitine treatment, tumors in control animals reached a volume thrice the original in ~2 days, whereas it took ~10 days for the tumors in treated animals to triplicate their initial volume (Fig. 5A). Overall, this difference indicated that roscovitine treatment resulted in an ~5-fold reduction in tumor growth.

It is important to point out that roscovitine seemed to be particularly effective against ESFT cells, relative to other human tumor cell types, both in culture and in nude mouse xenografts. Our working concentration in culture (10 μmol/L) compares favorably with the reported IC₅₀ values for cytotoxicity of roscovitine on a variety of human tumor and untransformed cell lines (19, 23–26). Furthermore, and most importantly, treatment for 5 consecutive days with only one i.p. injection at 50 mg/kg/d (total roscovitine dose of 250 mg/kg) reduced tumor size, relative to untreated control animals, by ~85% (days 5–8; Fig. 5A), whereas treatment schedules including three daily i.p. injections at 100 mg/kg/d for 5 days (total dose of 1,500 mg/kg) were reported to reduce by only 45% and 62%, respectively, the growth of tumors induced in nude mice with human colon (LoVo) and uterine (MESSA-DX5) tumor cell lines (19). The fact that our treatment achieved a better antitumor response with 6-fold lower total doses strongly indicates that roscovitine is substantially more efficient

Figure 5. Roscovitine treatment of established ESFT xenografts results in tumor growth delay mediated by the induction *in vivo* of an apoptotic process that involves caspase-3 activation. **A**, xenografts established by s.c. inoculation of A4573 cells in mice were grown to a mean volume of 130 mm³. Animals were randomized into two groups. One group (*n* = 6) was treated with roscovitine, administered as single daily i.p. injections (arrows), at a dose of 50 mg/kg, for either 5 days or two 5-day series with a 2-day break in between. The control group (*n* = 6) received i.p. injections of the carrier solutions following identical schedules. Results shown correspond to one of the experimental replicas using the two 5-day treatment schedule. Tumor growth in roscovitine-treated animals was markedly slower than the growth of tumors in control animals, in agreement with the much smaller size (*inset*) of tumors excised from individual control or roscovitine-treated animals. Asterisks indicate that the differences observed in tumor growth were statistically significant (*P* = 0.001). **B**, control and roscovitine-treated mice were euthanized at different times after the first roscovitine injection for up to several weeks after completion of the treatment. At those times, tumors were removed, measured, stained with H&E, and examined for evidence of apoptosis by *in situ* TUNEL assays and immunohistochemistry with an anti-cleaved caspase-3 specific antibody. Data from the analysis of tumors excised 7 days after the first roscovitine injection are shown. Results indicated that roscovitine efficiently induced apoptosis of ESFT cells *in vivo*.



against ESFT than against other human tumor cells. These results showed that roscovitine efficiently inhibited ESFT cell growth *in vivo* as well as in culture. To further elucidate the mechanism of roscovitine action *in vivo*, we examined whether tumor tissues showed any evidence of apoptosis. As shown in Fig. 5B, results from both TUNEL assays (Fig. 5B, middle) and immunohistochemical detection of cleaved caspase-3 (Fig. 5B, right) showed that roscovitine also induced apoptosis of ESFT tumors *in vivo* by a caspase-dependent mechanism. In contrast, negligible signs of apoptosis were detectable in tumors from control animals (Fig. 5B, top) injected with carrier solution alone.

The present study provides the first description that ESFT cells are uniformly sensitive to roscovitine both *in vitro* and *in vivo*. It has been reported that roscovitine induced apoptotic cell death in maturing cerebellar granule neurons (40). However, it seems likely that these data may be a consequence of an increased sensitivity of rat primary cells in culture rather than a reflection of a universal sensitivity of normal human cells to roscovitine. Indeed, reports from clinical trials (19–22) consistently indicated that roscovitine showed very low toxicity in phase Ib clinical trials and that it is now entering phase II trials. Taking this into consideration, along with reports on the selectivity of roscovitine for rapidly prolifer-

ating over nonproliferating cells (19, 41), our data also provide the basis for a new promising approach for the management of ESFT either as a single treatment or in combination with other therapeutic modalities. In fact, enhanced apoptotic induction has been previously shown *in vitro* and *in vivo* using roscovitine in combination with either *E2F-1* gene therapy for gastric and pancreatic cancers (42, 43), with ionizing radiation on human breast carcinoma (32), or with certain chemotherapeutic drugs on glioma (33) or bladder and prostate carcinoma (44). Overall, our results strongly suggest that roscovitine may be an effective therapeutic agent against ESFT, alone or in combination with other potentially synergistic treatments, and support its inclusion in ESFT treatment protocols.

Acknowledgments

Received 4/12/2005; revised 7/20/2005; accepted 8/2/2005.

Grant support: USPHS grant P01-CA74175 from the National Cancer Institute, NIH, and the Microscopy and Imaging Macromolecular Analysis and the Flow Cytometry/Cell Sorting Shared Resources of the Lombardi Comprehensive Cancer Center, funded through USPHS grant 2P30-CA51008.

The costs of publication of this article were defrayed in part by the payment of page charges. This article must therefore be hereby marked *advertisement* in accordance with 18 U.S.C. Section 1734 solely to indicate this fact.

References

- Arvand A, Denny CT. Biology of EWS/ETS fusions in Ewing's family tumors. *Oncogene* 2001;20:5747–54.
- Kolb EA, Kushner BH, Gorlick R, et al. Long-term event-free survival after intensive chemotherapy for Ewing's family of tumors in children and young adults. *J Clin Oncol* 2003;21:3423–30.
- Van Valen F, Fulda S, Truckenbrod B, et al. Apoptotic responsiveness of the Ewing's sarcoma family of tumours to tumour necrosis factor-related apoptosis-inducing ligand (TRAIL). *Int J Cancer* 2000;88:252–9.
- Mateo-Lozano S, Tirado OM, Notario V. Rapamycin induces the fusion-type independent downregulation of the EWS/FLI-1 proteins and inhibits Ewing's sarcoma cell proliferation. *Oncogene* 2003;22:9282–7.
- Malumbres M, Barbacid M. To cycle or not to cycle: a critical decision in cancer. *Nat Rev Cancer* 2001;1:222–31.
- Knockaert M, Greengard P, Meijer L. Pharmacological inhibitors of cyclin-dependent kinases. *Trends Pharmacol Sci* 2002;23:417–25.
- Baer C, Nees M, Breit S, et al. Profiling and functional annotation of mRNA gene expression in pediatric rhabdomyosarcoma and Ewing's sarcoma. *Int J Cancer* 2004;110:687–94.
- Zhang J, Hu S, Schofield DE, Sorensen PHB, Triche TJ. Selective usage of D-type cyclins by Ewing's tumors and rhabdomyosarcomas. *Cancer Res* 2004;64:6026–34.
- Schaefer KL, Brachwitz K, Wai DH, et al. Expression profiling of t(12;22) positive clear cell sarcoma of soft tissue cell lines reveals characteristic up-regulation of potential new marker genes including *ERBB3*. *Cancer Res* 2004;64:3395–405.
- Staeger MS, Hutter C, Neumann I, et al. DNA microarrays reveal relationship of Ewing family tumors to both endothelial and fetal neural crest-derived cells and define novel targets. *Cancer Res* 2004;64:8213–21.
- Ohali A, Avigad S, Zaizov R, et al. Prediction of high risk Ewing's sarcoma by gene expression profiling. *Oncogene* 2004;23:8997–9006.
- Kovar H, Jug G, Aryee DNT, et al. Among genes involved in the *RB* dependent cell cycle regulatory cascade, the *p16* tumor suppressor gene is frequently lost in the Ewing family of tumors. *Oncogene* 1997;15:2225–32.
- Dauphinot L, De Oliveira C, Melot T, et al. Analysis of the expression of cell cycle regulators in Ewing cell lines: EWS-FLI-1 modulates p57^{KIP2} and c-Myc expression. *Oncogene* 2001;20:3258–65.
- Fukuma M, Okita H, Hata J, Umezawa A. Upregulation of Id2, an oncogenic helix-loop-helix protein, is mediated by the chimeric EWS/ets protein in Ewing sarcoma. *Oncogene* 2003;22:1–9.
- López-Guerrero JA, Pellin A, Noguera R, Carda C, Llombart-Bosch A. Molecular analysis of the *9p21* locus and *p53* genes in Ewing family tumors. *Lab Invest* 2001;81:803–14.
- Burchill SA. Ewing's sarcoma: diagnostic, prognostic, and therapeutic implications of molecular abnormalities. *J Clin Pathol* 2003;56:96–102.
- Whittaker SR, Walton MI, Garrett MD, Workman P. The cyclin-dependent kinase inhibitor CYC202 (Roscovitine) inhibits retinoblastoma protein phosphorylation, causes loss of Cyclin D1, and activates the mitogen-activated protein kinase pathway. *Cancer Res* 2004;64:262–72.
- Maude SL, Enders GH. Cdk inhibition in human cells compromises Chk1 function and activates a damage response. *Cancer Res* 2005;65:780–6.
- McClue SJ, Blake D, Clarke R, et al. *In vitro* and *in vivo* antitumor properties of the cyclin dependent kinase inhibitor CYC202 (R-roscovitine). *Int J Cancer* 2002;102:463–8.
- Fischer PM, Gianella-Borradori A. CDK inhibitors in clinical development for the treatment of cancer. *Expert Opin Investig Drugs* 2003;12:955–70.
- Senderowicz AM. Novel small molecule cyclin-dependent kinases modulators in human clinical trials. *Cancer Biol Ther* 2003;2:S84–95.
- De la Motte S, Gianella-Borradori A. Pharmacokinetic model of R-roscovitine and its metabolite in healthy male subjects. *Int J Clin Pharmacol Ther* 2004;42:232–9.
- Wojciechowski J, Horky M, Gueorguieva M, Węsierska-Gądek J. Rapid onset of nucleolar disintegration preceding cell cycle arrest in roscovitine-induced apoptosis of human MCF-7 breast cancer cells. *Int J Cancer* 2003;106:486–95.
- Hahtow IN, Schneller F, Oelsner M, et al. Cyclin-dependent kinase inhibitor Roscovitine induces apoptosis in chronic lymphocytic leukemia cells. *Leukemia* 2004;18:747–55.
- MacCallum DE, Melville J, Frame S, et al. Seliciclib (CYC202, R-Roscovitine) induces cell death in multiple myeloma cells by inhibition of RNA polymerase II-dependent transcription and down-regulation of Mcl-1. *Cancer Res* 2005;65:5399–407.
- Węsierska-Gądek J, Gueorguieva M, Horky M. Roscovitine-induced up-regulation of p53/AIP1 protein precedes the onset of apoptosis in human MCF-7 breast cancer cells. *Mol Cancer Ther* 2005;4:113–24.
- Matsumoto Y, Tanaka K, Nakatani F, Matsunobu T, Matsuda S, Iwamoto Y. Downregulation and forced expression of EWS-Flil fusion gene results in changes in the expression of G₁ regulatory genes. *Br J Cancer* 2001;84:768–75.
- Nakatani F, Tanaka K, Sakimura R, et al. Identification of p21WAF1/CIP1 as a direct target of EWS-Flil oncogenic fusion protein. *J Biol Chem* 2003;278:15105–15.
- Ribas J, Boix J. Cell differentiation, caspase inhibition, and macromolecular synthesis blockage, but not BCL-2 or BCL-XL proteins, protect SH-SY5Y cells from apoptosis triggered by two CDK inhibitory drugs. *Exp Cell Res* 2004;295:9–24.
- Mgbonyebi OP, Russo J, Russo IH. Roscovitine induces cell death and morphological changes indicative of apoptosis in MDA-MB-231 breast cancer cells. *Cancer Res* 1999;59:1903–10.
- Edamatsu H, Gau CL, Nemoto T, Guo L, Tamanoi F. Cdk inhibitors, roscovitine and olomoucine, synergize with farnesyltransferase inhibitor (FTI) to induce efficient apoptosis of human cancer cell lines. *Oncogene* 2000;19:3059–68.
- Maggiorella L, Deutsch E, Frascogna V, et al. Enhancement of radiation response by roscovitine in human breast carcinoma *in vitro* and *in vivo*. *Cancer Res* 2003;65:2513–7.
- Kim EH, Kim SU, Shin DY, Choi KS. Roscovitine sensitizes glioma cells to TRAIL-mediated apoptosis by downregulation of survivin and XIAP. *Oncogene* 2004;23:446–56.
- Mihara M, Shintani S, Nakashiro K, Hamakawa H. Flavopiridol, a cyclin dependent kinase (CDK) inhibitor, induces apoptosis by regulating Bcl-x in oral cancer cells. *Oral Oncol* 2003;39:49–55.
- Siddik ZH. Cisplatin: mode of cytotoxic action and molecular basis of resistance. *Oncogene* 2003;22:7265–79.
- Yen HC, Tang YC, Chen FY, Chen SW, Majima HJ. Enhancement of cisplatin-induced apoptosis and caspase 3 activation by depletion of mitochondrial DNA in a human osteosarcoma cell line. *Ann N Y Acad Sci* 2005;1042:516–22.
- Blaydes JP, Craig AL, Wallace M, et al. Synergistic activation of p53-dependent transcription by two

- cooperating damage recognition pathways. *Oncogene* 2000;19:3829–39.
38. Alvi AJ, Austen B, Weston VJ, et al. A novel CDK inhibitor, CYC202 (R-roscovitine), overcomes the defect in p53-dependent apoptosis in B-CLL by down-regulation of genes involved in transcription regulation and survival. *Blood* 2005;105:4484–91.
39. Tirado OM, Mateo-Lozano S, Notario V. Rapamycin induces apoptosis of JN-DSRCT-1 cells by increasing the Bax: Bcl-xL ratio through concurrent mechanisms dependent and independent of its mTOR inhibitory activity. *Oncogene* 2005;24:3348–57.
40. Monaco EA III, Beaman-Hall CM, Mathur A, Vallano ML. Roscovitine, olomucine, purvalanol: inducers of apoptosis in maturing cerebellar granule neurons. *Biochem Pharmacol* 2004;67:1947–64.
41. Atanasova G, Jans R, Zhelev N, Mitev V, Poumay Y. Effects of cyclin-dependent kinases inhibitor CYC202 (R-roscovitine) on the physiology of cultured human keratinocytes. *Biochem Pharmacol* 2005;70:824–36.
42. Atienza C, Jr., Elliott MJ, Dong YB, et al. Adenovirus-mediated *E2F-1* gene transfer induces an apoptotic response in human gastric carcinoma that is enhanced by cyclin dependent kinase inhibitors. *Int J Mol Med* 2000;6:55–63.
43. Elliott MJ, Farmer MR, Atienza C, Jr., et al. *E2F-1* gene therapy induces apoptosis and increases chemosensitivity in human pancreatic carcinoma cells. *Tumour Biol* 2002;23:76–86.
44. Lashinger LM, Zhu K, Williams SA, Shrader M, Dinney CPN, McConkey DJ. Bortezomib abolishes tumor necrosis factor-related apoptosis inducing ligand resistance via a p21 dependent mechanism in human bladder and prostate cancer cells. *Cancer Res* 2005;65:4902–8.

Cancer Research

The Journal of Cancer Research (1916–1930) | The American Journal of Cancer (1931–1940)

Roscovitine Is an Effective Inducer of Apoptosis of Ewing's Sarcoma Family Tumor Cells *In vitro* and *In vivo*

Oscar M. Tirado, Silvia Mateo-Lozano and Vicente Notario

Cancer Res 2005;65:9320-9327.

Updated version Access the most recent version of this article at:
<http://cancerres.aacrjournals.org/content/65/20/9320>

Cited articles This article cites 44 articles, 13 of which you can access for free at:
<http://cancerres.aacrjournals.org/content/65/20/9320.full#ref-list-1>

Citing articles This article has been cited by 7 HighWire-hosted articles. Access the articles at:
<http://cancerres.aacrjournals.org/content/65/20/9320.full#related-urls>

E-mail alerts [Sign up to receive free email-alerts](#) related to this article or journal.

Reprints and Subscriptions To order reprints of this article or to subscribe to the journal, contact the AACR Publications Department at pubs@aacr.org.

Permissions To request permission to re-use all or part of this article, use this link
<http://cancerres.aacrjournals.org/content/65/20/9320>.
Click on "Request Permissions" which will take you to the Copyright Clearance Center's (CCC) Rightslink site.